Theory of potential modulation in lateral surface superlattices.   II.   Piezoelectric effect

Ivan A. Larkin* and John H. Davies[†]

Department of Electronics and Electrical Engineering, Glasgow University, Glasgow, G12 8QQ, United Kingdom

Andrew R. Long

Department of Physics and Astronomy, Glasgow University, Glasgow, G12 8QQ, United Kingdom

Ramon Cuscó

Institut Jaume Almera, Consell Superior d'Investigacions Científiques (CSIC), Lluís Solé i Sabarís s.n., 08028 Barcelona, Spain

We have calculated the piezoelectric coupling between a two-dimensional electron gas and the stress field due to a lateral surface superlattice, a periodic striped gate. Stress is assumed to arise from differential contraction between the metal gate and semiconductor. The piezoelectric potential is several times larger than the deformation potential and generally gives the dominant coupling. It depends on the orientation of the device and vanishes on a (100) surface if the current flows parallel to a crystallographic axis. Most devices, however, are fabricated parallel to {011} cleavage planes in which case the piezoelectric potential is at a maximum. There are several sources of screening, including the partly occupied donors in a typical GaAs-Al$_x$Ga$_{1-x}$As heterostructure. We also consider different elastic models for the gate. The best agreement with experiment is obtained if the force is distributed over the interface between the gate and semiconductor, rather than being concentrated at its ends. [S0163-1829(97)03440-1]

I. INTRODUCTION

The high mobility of electrons in a two-dimensional electron gas (2DEG) in a heterostructure has made it the foundation for a huge range of experiments[1] in which the mean free path or wavelength of the electrons is comparable with the size of a device. Often the electrons are guided by metal gates on the surface, and it is assumed that the electrons are influenced only by the electrostatic field from the bias on these gates. This hypothesis can be tested by experiments that measure the potential in the 2DEG, and commensurability oscillations in a magnetic field[2–4] provide a convenient tool. These detect the periodic potential under a lateral surface superlattice, a device with a sequence of equally-spaced parallel metal gates perpendicular to the flow of current between source and drain. The potential can be deduced from a straightforward analysis of the magnetoresistance.[4–6]

An experiment[7] that used a lateral surface superlattice on a particularly shallow 2DEG showed a periodic potential even when the gates were grounded. There was also a strong second harmonic. In a previous paper,[8] which we shall refer to as paper I, we considered possible sources of this modulation. We were unable to reproduce the harmonic content of the measured potential assuming a built-in voltage on the gates. Instead we proposed that differential contraction between the gate and semiconductor led to strain which caused the observed modulation of the 2DEG. It is now recognized[9] that strain plays a role in many experiments where electronic transport is sensitive to weak potentials.

We assumed in paper I that strain coupled to the 2DEG through the deformation potential. This gave good qualitative agreement with experiment and explained the strong second harmonic observed. However, the magnitude was too small by nearly an order of magnitude when all sources of screening were taken into account, including a parasitic layer of electrons around the donors in the experimental structure.

Strain also couples to electrons through the piezoelectric effect in III–V semiconductors. This interaction depends on orientation unlike the deformation potential. Most samples are grown on (100) surfaces and we assumed in paper I that the current flowed along the [010] direction. There is no piezoelectric interaction in this case. Practical devices, however, are usually oriented parallel to the {011} cleavage planes, and current flows along a ⟨011⟩ direction. This maximizes the piezoelectric coupling and the potentials calculated in paper I are therefore incomplete for most experiments. This paper corrects that omission by including the piezoelectric interaction. We shall also improve other aspects of the physical model, particularly with respect to the boundary conditions applied to the electrostatic and elastic fields. Thus our aims are as follows.

(1) To calculate the piezoelectric potential as a function of orientation and compare its magnitude with that from the deformation potential.
(2) To clarify the boundary conditions for the electrostatic problem, particularly the role of surfaces and doped regions.
(3) To consider different elastic models for the gate.

It has been realized for some time that stress is induced during the manufacture of field-effect transistors (FET's). In a landmark paper, Asbeck *et al.*[10] showed that the resulting piezoelectric potential had a measurable effect on the threshold voltage of FET's. A signature of the piezoelectric effect is its dependence on orientation, with opposite signs for current along [011] and [01$\bar{1}$]. We shall extend their results to a superlattice and calculate in more detail the potential seen by
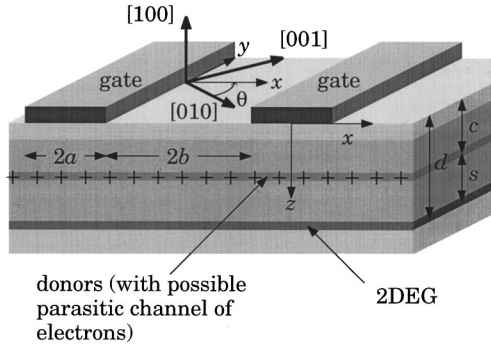
FIG. 1. Construction and orientation of the lateral surface superlattice used in the experiment. The donors lie in a plane c below the surface. The 2DEG lies a further distance s below the donors (which includes an allowance for the thickness of the 2DEG). The lengths of the gates and gaps are $2a$ and $2b$ with the origin in the center of a gate. The crystal axis (100) is an upward normal to the surface, opposite to z which points down into the substrate. The current flows along x which makes an angle θ with [010].

the electrons. Piezoelectric effects have also been seen in resonant-tunneling devices,[11] where the peak in $I(V)$ could be moved in opposite directions by the application of stress along [011] or [01$\bar{1}$].

There are several important differences between the modulations induced by the piezoelectric effect and the deformation potential.

(1) The piezoelectric effect depends on orientation but the deformation potential does not, within the isotropic approximation for the elastic constants.
(2) The piezoelectric effect is several times larger for samples in the usual orientation.
(3) They are affected by screening in different ways. In particular, the piezoelectric charge extends *deeper* than the 2DEG where it is less affected by screening due to surface states or electrons around the donors.
(4) The shape of the piezoelectric potential changes dramatically with the ratio of the period of the superlattice to the depth of the 2DEG; the deformation potential is less sensitive.

We shall first review the calculation of the elastic field, using three models of the gate. These differ in the distribution of force over the interface between the gate and semiconductor and apply to gates of different thickness. Next we calculate the potential due to the piezoelectric interaction. This includes the effect of orientation and screening by regions of the structure which are often considered inert, such as the surface and doped layer. Finally, we compare our results with experiments on lateral surface superlattices. We are now able to explain the observed magnitude[7] of the periodic potential. The harmonic content is also in agreement; it reflects the elastic behavior of the gate, but is also sensitive to the precise dimensions of the structure. A recent experiment[12] has verified the piezoelectric origin of the potential through its dependence on orientation.

We made an unfortunate choice of axes in paper I which we have changed to avoid confusion here, where a precise description of the orientation is essential. Figure 1 shows the crystallographic axes for the conventional setting of a (100)

wafer and the orientation of the device. We choose z directed down into the substrate and x along the direction of current, with the origin in the center of a gate. The current and x axis make an angle θ with the [010] direction. There is translational invariance along y, parallel to the width of the gates of the superlattice.

The figure also shows the geometry of the superlattice, for which we shall use parameters to match the device[7] studied in paper I. The layers comprised a GaAs substrate, two 10 nm thick AlAs barriers separated by 2 nm of $Al_xGa_{1-x}As$ δ-doped with Si to 4×10^{16} m^{-2}, and a 5.4 nm GaAs cap layer. The 2DEG was confined at an interface 28 nm deep. The extent of the wave function normal to this interface was about 7–8 nm, which is much smaller than the period of the superlattice. We shall therefore treat it simply by adding its thickness to the depth of the 2DEG. Thus the donors are at a depth $c \approx 17$ nm, separated from the the 2DEG by a spacer $s \approx 18$ nm, which gives an overall depth $d = c + s \approx 35$ nm. The gates were deposited as 15 nm Ti followed by 15 nm Au, giving a thickness $h = 30$ nm. Their length was $2a = 130$ nm and the gaps were $2b = 140$ nm, with the origin in the center of a gate. The presence of the donors will be important when we impose boundary conditions on the electrostatic problem arising from the piezoelectric charge density. A complication of this particular device is that it showed a low density of mobile electrons around the donors even at low temperature[13] because of the AlAs barriers.

II. ELASTIC PROBLEM

The first task is to calculate the elastic field generated by the gate. We proposed in paper I that stress arose from differential contraction between each gate on the surface and the underlying semiconductor. A patterned, strained layer on the surface could be treated in the same way. The elastic problem is to calculate the stress that this causes throughout the semiconductor. An accurate treatment would require numerical solution of the elastic equations but, for the results to be meaningful, would also need a good description of the interface between the gate and semiconductor. Little information about this interface is available. Rather than take a numerical approach, we shall study some simple models analytically. These are chosen to encompass the likely range of behavior in real devices.

Several simplifications were made in paper I to render the problem practicable. First, the differences in elastic constants between GaAs and AlAs were ignored and we treated the material as isotropic. The problem becomes much more complicated if we relax these simplifications and we shall therefore retain them. Second, we assumed that the gate was very ''wide'' along y. Displacement along y will then be confined to the extremities of the gate and we can assume that most of the system is in a plane state of strain in the x-z plane. It is implicit that the gate covers too small an area to induce macroscopic bending of the sample. Thus $\varepsilon_{yy} = \varepsilon_{xy} = \varepsilon_{yz} = 0$ and the shear stresses σ_{xy} and σ_{yz} also vanish, but $\sigma_{yy} \neq 0$. Standard elastic theory[14] then shows that the stress in our two-dimensional problem can be deduced from a biharmonic Airy stress function χ. The components in the xz plane are given by

$$\sigma_{xx} = \frac{\partial^2 \chi}{\partial z^2}, \quad \sigma_{xz} = -\frac{\partial^2 \chi}{\partial x \partial z}, \quad \sigma_{zz} = \frac{\partial^2 \chi}{\partial x^2}. \quad (2.1)$$

Setting $\varepsilon_{yy} = 0$ and eliminating σ_{yy} from the usual relation between normal stress and strain gives $E\varepsilon_{xx}(x,z) = (1-\nu^2)\sigma_{xx}(x,z) - \nu(1+\nu)\sigma_{zz}(x,z)$ and similarly for ε_{zz}, where E and ν are Young's modulus and Poisson's ratio for the semiconductor.

The gate is likewise in a plane state of strain and we also take it to be thin, $h \ll a$. It is then reasonable to assume further that the stress and strain are independent of z through the thickness of the gate. In particular, as $\sigma_{zz}^{\text{gate}} = 0$ on the exposed top surface, this is taken to hold throughout the gate. The normal stress and strain along x, the length of the gate, are then related by $E_{\text{gate}}\varepsilon_{xx}^{\text{gate}}(x) = (1-\nu_{\text{gate}}^2)\sigma_{xx}^{\text{gate}}(x)$.

A. Compatibility between gate and semiconductor

We must now set up equations relating the elastic fields in the gate and the surface of the semiconductor in the plane $z = 0$. The general equation relating stress to applied force is $\mathbf{F} = -\text{div } \boldsymbol{\sigma}$ with a body force $\mathbf{F}$ per unit volume. This becomes $\mathbf{P} = \boldsymbol{\sigma} \cdot \hat{\mathbf{n}}$ at a surface where $\mathbf{P}$ is the force per unit area and $\hat{\mathbf{n}}$ is an outward unit normal. (These relations are analogous to $\rho = -\text{div } \mathbf{P}$ and $\sigma = \mathbf{P} \cdot \hat{\mathbf{n}}$ for the electrostatic polarization field.) On the exposed surface of the semiconductor between the gates this gives $\sigma_{xz} = \sigma_{zz} = 0$. We have assumed that $\sigma_{zz}^{\text{gate}} = 0$ because the gate is thin and $\sigma_{zz} = 0$ therefore holds over the whole surface of the semiconductor. The biharmonic potential χ can then be written as $\chi = z\phi$, where $\nabla^2 \phi = 0$. This is equivalent to an electrostatic problem and we shall make frequent use of the analogy.

The remaining stress $\sigma_{xx}^{\text{gate}}$ in the gate exerts a force per unit area $P_x(x)$ on the semiconductor underneath. We have assumed the stress to be constant through the thickness h of the gate, so its body force integrates to $P_x(x) = h d\sigma_{xx}^{\text{gate}}/dx$; the sign accounts for this being a force exerted by the gate on the semiconductor. This in turn generates a shear stress on the semiconductor whose value at the surface is $\sigma_{xz}(x,z=0) = -P_x(x)$; there is a minus sign because our z-axis points into the semiconductor. Thus the stresses in the gate and semiconductor are related by

$$\sigma_{xz}(x,z=0) = -P_x(x) = -h\frac{d\sigma_{xx}^{\text{gate}}}{dx}. \quad (2.2)$$

Our picture is that the stress arises from differential thermal contraction. For definiteness, suppose that the whole system is initially undistorted and stress free at some constant temperature throughout. Now raise the temperature of the gate alone through ΔT. The effect of this can be incorporated into the elastic equations for the gate[14] by changing the normal stresses so that $\sigma_{xx}^{\text{gate}} \to \sigma_{xx}^{\text{gate}} + \alpha_{\text{gate}}E_{\text{gate}}\Delta T/(1-2\nu_{\text{gate}})$ and similarly for y and z, where α_{gate} is the gate's coefficient of linear expansion. The stress and strain along x within the gate then obey

$$E_{\text{gate}}\varepsilon_{xx}^{\text{gate}}(x) = (1-\nu_{\text{gate}}^2)\sigma_{xx}^{\text{gate}}(x) + (1+\nu_{\text{gate}})E_{\text{gate}}\alpha_{\text{gate}}\Delta T. \quad (2.3)$$

The resulting distortion along x is transmitted identically to the semiconductor, assuming perfect bonding, so $\varepsilon_{xx}(x,z=0) = \varepsilon_{xx}^{\text{gate}}(x)$. This relation, together with Eqs. (2.2) and (2.3), gives

$$\frac{1-\nu^2}{E}\sigma_{xx}(x,z=0) + \frac{1-\nu_{\text{gate}}^2}{hE_{\text{gate}}}\int_0^x \sigma_{xz}(x',z=0)dx'$$
$$= (1+\nu_{\text{gate}})\alpha_{\text{gate}}\Delta T. \quad (2.4)$$

This is the compatibility relation for the stresses under the gate. In our problem $\alpha_{\text{gate}}\Delta T$ should be replaced by the differential contraction of the gate with respect to the semiconductor, about -0.001. Equation (2.4) is effectively an integral equation for the potential ϕ and can be solved numerically. Alternatively, a semi-infinite gate with a single edge can be treated with the Wiener-Hopf technique. We shall instead consider some simple limits of this equation.

1. Thick gate—"rigid" model

The second term on the left-hand side of Eq. (2.4) can be neglected if $h \gg a$. This leads to a uniform lateral strain ε_{xx}^0 and stress $\sigma_{xx}^0 = \varepsilon_{xx}^0 E/(1-\nu^2)$ on the surface under the gate, given by $\varepsilon_{xx}^0 = (1+\nu_{\text{gate}})\alpha_{\text{gate}}\Delta T$. This is almost the obvious result from thermal expansion of the gate imposing itself on the semiconductor underneath; the factor of $(1+\nu_{\text{gate}})$ appears because the gate is clamped along y. We used this model in paper I and shall call it a "rigid" gate. It provides a consistent solution of the compatibility relation (2.4), but the condition $h \gg a$ describes a thick gate rather than a thin one as we have assumed.

2. Thin gate—"elastic" model

It is tempting in the opposite limit of a thin gate, $h \ll a$, to neglect the first term on the left-hand side of Eq. (2.4). This corresponds to a uniform stress in the gate of $\sigma_{xx}^{0,\text{gate}} = -E_{\text{gate}}\alpha_{\text{gate}}\Delta T/(1-\nu_{\text{gate}})$. In turn this exerts a force on the underlying semiconductor which is concentrated at the ends of the gate:

$$\sigma_{xz}(x,z=0) = -P_x(x) = -F_x^0[\delta(x-a) - \delta(x+a)]. \quad (2.5)$$

The force per unit length at each end is

$$F_x^0 = -h\sigma_{xx}^{0,\text{gate}} = \frac{hE_{\text{gate}}\alpha_{\text{gate}}\Delta T}{1-\nu_{\text{gate}}}, \quad (2.6)$$

which is proportional to the thickness of the gate. This approach was taken by Asbeck et al.,[10] drawing on earlier work of Kirkby et al.[15] and Blech and Meieran.[16] The physical picture is that the thin gate is prevented from expanding by the semiconductor underneath, and instead develops a uniform compressive stress $\sigma_{xx}^{0,\text{gate}}$. We shall therefore call this an "elastic" gate. The stress acts back on the semiconductor and leads to displacements which must be small if the approximation is to be consistent. Unfortunately, the solution of the elastic equations shows that the displacement diverges logarithmically at the edges of the gate. The solution is therefore inapplicable to these regions, but we appeal to St. Venant's principle[17] and use it where the distance from the edges of the gates is large compared with h.

3. Linear force model

The force between gate and semiconductor diverges at the edges of the gate in both models discussed above. The force under an elastic gate is concentrated into a δ-function, which is obviously unrealistic and could be spread over a length of roughly the thickness of the gate.[18] The force exerted by the rigid gate is less singular but diverges as an inverse square root. A model where the force remains finite would be attractive. The force is an odd function of position under the gate, so $P_x(x) \propto x$ is an obvious choice, corresponding to a parabolic profile for $\sigma_{xx}^{\text{gate}}(x)$. This model does not eliminate all the undesirable features: the step in $\sigma_{xz}(x,z=0)$ at each edge of the gate generates a logarithmic divergence in $\sigma_{xx}(x,z=0)$, and there is a band near the outside of each gate where $\sigma_{xx}(x,z=0)$ changes sign, entering compression rather than extension. However, this model may provide a useful check on any extreme behavior introduced by the rigid or elastic gates.

B. Elastic potentials

The next step is to calculate the elastic potential needed to describe each of the above types of gate. It is convenient to choose ϕ as the imaginary part of a complex potential $w = \xi + i\phi$, which is a function of the complex coordinate $\zeta = x + iz$. The stresses on the surface of the semiconductor (other terms appear when $z \neq 0$) are given by

$$\sigma_{xx}(x,z=0) = 2\frac{\partial \phi}{\partial z} = 2\frac{\partial \xi}{\partial x},$$

$$\sigma_{xz}(x,z=0) = -P_x(x) = -\frac{\partial \phi}{\partial x}. \quad (2.7)$$

It is also useful to note that

$$\sigma_{xx}^{\text{gate}}(x) = \frac{\phi(x,z=0)}{h}, \quad u_x(x,z=0) = \frac{2(1-\nu^2)\xi(x,z=0)}{E}. \quad (2.8)$$

The compatibility relation (2.4) can be written in terms of the potentials on $z=0$ as

$$\frac{2(1-\nu^2)}{E}\frac{\partial \xi}{\partial x} - \frac{1-\nu_{\text{gate}}^2}{hE_{\text{gate}}}\phi(x,z=0) = (1+\nu_{\text{gate}})\alpha_{\text{gate}}\Delta T. \quad (2.9)$$

The Kramers-Kronig relations allow this to be written as an integral equation for ϕ or ξ.

We shall now find ϕ for the three models of the gates. In all cases there is no shear stress on the surface between the gates. Equation (2.7) shows that ϕ must be constant in these regions and it is convenient to set it to zero.

1. Rigid gate

In this model there is a constant lateral stress σ_{xx}^0 under the gate, giving $\partial\phi/\partial z = \frac{1}{2}\sigma_{xx}^0$. In the electrostatic analogy for ϕ this corresponds to a constant charge density under each gate with zero potential between them. This is a well-known mixed boundary value problem whose solution for an array of gates was obtained by conformal transformation in paper I. Put $Z = \pi\zeta/(a+b)$ and $A = \pi a/(a+b)$ for brevity. Then

$$w_{\text{rigid}}(\zeta) = \frac{\sigma_{xx}^0}{2}\frac{a+b}{\pi}\left[Z - 2\arccos\frac{\cos\frac{1}{2}Z}{\cos\frac{1}{2}A}\right]. \quad (2.10)$$

The solution of Poisson's equation for the piezoelectric charge is simplified if we exploit the periodic nature of the superlattice and use a Fourier series. This also facilitates comparison with experiment, which gives only the squared modulus of the Fourier coefficients. The harmonic function ϕ can be expanded as

$$\phi(x,z) = \sum_{n=0}^{\infty} \phi_n \cos(q_n x)\exp(-q_n z), \quad (2.11)$$

where the wave vectors $q_n = \pi n/(a+b)$. It is easier to start from the derivative for the rigid gate,

$$\frac{dw_{\text{rigid}}}{d\zeta} = \frac{\sigma_{xx}^0}{2}\left[1 - \frac{\sin\frac{1}{2}Z}{\sqrt{\sin^2\frac{1}{2}Z - \sin^2\frac{1}{2}A}}\right]. \quad (2.12)$$

Expansion of the trigonometric functions as complex exponentials gives

$$\frac{dw_{\text{rigid}}}{d\zeta} = \frac{\sigma_{xx}^0}{2}\left[1 + \frac{e^{iZ}-1}{\sqrt{1-2e^{iZ}\cos A + e^{2iZ}}}\right]. \quad (2.13)$$

We recognize the square root as the generating function for Legendre polynomials. Using this expansion, integrating to return to w, and taking the imaginary part finally leads to coefficients

$$\phi_n^{\text{rigid}} = \frac{\sigma_{xx}^0}{2}\frac{a+b}{\pi}\frac{P_n(\cos A) - P_{n-1}(\cos A)}{n} \quad (2.14)$$

for $n>0$. We also find $\phi_0^{\text{rigid}} = \sigma_{xx}^0[(a+b)/\pi]\ln\cos A$ from the asymptotic expansion of $w_{\text{rigid}}(\zeta)$.

2. Elastic gate

The only shear stress on the surface of the semiconductor is at the edges of the gates in this model, and Eq. (2.7) shows that ϕ is therefore a piecewise constant function. Equation (2.5) is satisfied if

$$\phi_{\text{elastic}}(x,z=0) = \begin{cases} -F_x^0 & \text{under the gates,} \\ 0 & \text{elsewhere.} \end{cases} \quad (2.15)$$

Superposition is simple with this model because the potential is specified all over the surface, and it can readily be generalized. This is equivalent to an electrostatic problem where the potential is a square wave on the boundary. It can be extended for all z by standard methods[19] to give

$$w_{\text{elastic}} = -\frac{F_x^0}{\pi}\ln\frac{\sin\frac{1}{2}(Z-A)}{\sin\frac{1}{2}(Z+A)}. \quad (2.16)$$

A single gate can be treated by setting $b \to \infty$. The Fourier expansion is simple,

$$\phi_n^{\text{elastic}} = -(2F_x^0 \sin nA)/n\pi \qquad (2.17)$$

for $n > 0$, with $\phi_0^{\text{elastic}} = -aF_x^0/(a+b)$.

3. Sine force model

Complete solution of the model with a linear force gradient described in Sec. II A 3 proves troublesome for a periodic gate. We shall instead use a slightly different ''sine gate'' model in which the profile of the force follows part of a sine curve rather than a straight line. It has a complex potential

$$w_{\text{sine}}(\zeta) = C\left[A\,\sin Z + (\cos A - \cos Z)\ln \frac{\sin\frac{1}{2}(Z-A)}{\sin\frac{1}{2}(Z+A)} \right],$$
$$(2.18)$$

where C is a constant to be determined. The force exerted by the gate $P_x(x) = [\pi^2 C/(a+b)]\sin[\pi x/(a+b)]$. This returns to a linear profile as in Sec. II A 3 when $a \ll b$ and the gates are nearly isolated, but gives a sine wave for a continuous gate. Expansion of the complex potential as in Sec. II B 1, or direct integration, shows that the Fourier coefficients are

$$\phi_n^{\text{sine}} = -\frac{C}{n}\left[\frac{\sin(n-1)A}{n-1} - \frac{\sin(n+1)A}{n+1} \right]. \qquad (2.19)$$

The limit should be taken for $n = 1$ and $\phi_0^{\text{sine}} = -C(\sin A - A\cos A)$.

This model is only a rough solution to the compatibility relation (2.9), which leaves ambiguity in the choice of the prefactor C. One method would be to minimize the total elastic energy. We have taken the simpler route of integrating both sides of Eq. (2.9) across the gate and choosing C to satisfy this averaged relation, which gives

$$C = \frac{\varepsilon_{xx}^0}{\pi}\left[\frac{2(1-\nu^2)\sin A}{E(a+b)} + \frac{(1-\nu_{\text{gate}}^2)(\sin A - A\cos A)}{E_{\text{gate}}hA} \right]^{-1}.$$
$$(2.20)$$

This has the satisfying feature that $C \propto h$ for a thin gate and saturates for a thick gate, but it must be remembered that this model does not provide a consistent solution to the compatibility relation (2.9) in either limit.

C. Comparison of different models

Figure 2 shows the stress on the surface and gate according to the three elastic models for the gate. Assuming that differential contraction between Ti and GaAs was responsible for the strain, we estimated in paper I that the surface of the semiconductor was in compression of $\varepsilon_{xx}^0 = -0.001$ under a rigid gate. This figure may be subject to large errors as the precise conditions of deposition are uncertain. We use parameters for GaAs (Ref. 20) throughout the semiconductor of $E = 90$ GPa and $\nu = 0.31$, with $E^{\text{gate}} = 100$ GPa and $\nu^{\text{gate}} = 0.30$ for the gate. In general, the stress has a different magnitude in the three models because of their different dependence on the thickness of the gate; in this example, however, they are very similar.

The force $P_x(x)$ between the gate and semiconductor (thick line) has contrasting behavior in the three models. There is a δ function at each edge of the elastic gate (b) and
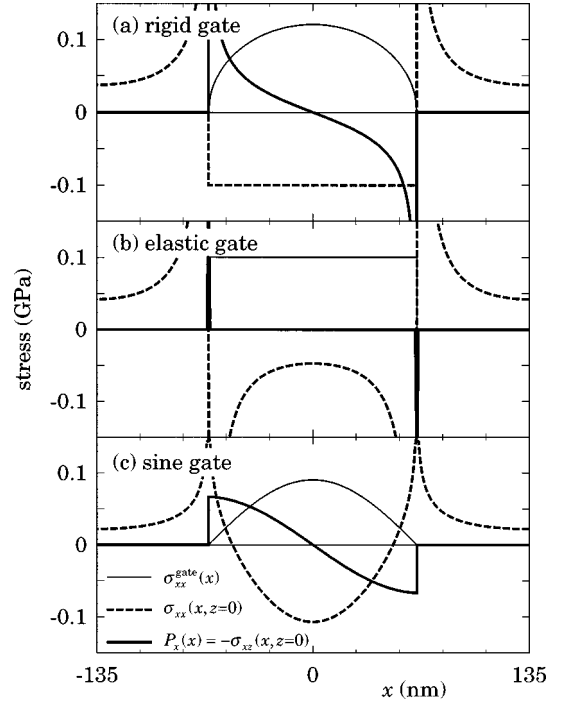
FIG. 2. Stresses according to the (a) rigid, (b) elastic, and (c) sine models of the gate. Thick line: force $P_x(x) = -\sigma_{xz}(x, z=0)$ exerted by the gate on the semiconductor; this reduces to δ-functions for the elastic gate. Broken line: lateral stress $\sigma_{xx}(x, z=0)$ in semiconductor at surface. Thin line: lateral stress $\sigma_{xx}^{\text{gate}}(x)$ in gate.

a square-root divergence in the rigid model (a), but the sine gate gives a well-behaved function (a half-cycle of a sine wave, as the name implies) in (c). Differential contraction puts the semiconductor into compression under the middle of each gate, and $\sigma_{xx}(x, z=0)$ is constant (dashed line) as expected under the rigid gate. The semiconductor is in lateral extension between the gates and the stress changes sign at the edges of a rigid or elastic gate. For a sine gate, however, $\sigma_{xx}(x, z=0)$ changes sign underneath the gate so there are strips under the outside of each gate where the semiconductor is in extension rather than compression. The stress $\sigma_{xx}^{\text{gate}}(x)$ within the gate (thin line) is constant for the elastic gate but drops to zero at the edges in the other models.

The Fourier expansions of ϕ also show different characteristics. These can be deduced from the figure, remembering that $\phi(x, z=0) = h\sigma_{xx}^{\text{gate}}(x)$ (thin curve). The experiment is close to the limit of equal gates and gaps where $A = \pi/2$. The even coefficients vanish in this limit for the elastic gate, and this should be reflected in the potential and magnetoresistance. There is no such cancellation for the rigid gate where all coefficients remain nonzero although $\cos A = 0$ and the odd Legendre polynomials vanish. The odd coefficients except $n = 1$ vanish for the sine gate. Thus the commensurability oscillations should be able to distinguish between these different models for the elastic behavior. This completes our solution of the elastic problem.

III. PIEZOELECTRIC POTENTIAL

We shall now use the stress to calculate the density of polarization charge from the piezoelectric effect, and inte-

grate Poisson's equation with this charge density to find the resulting potential energy in the 2DEG. Most of this is straightforward apart from the boundary conditions on the electrostatic potential.

A. Piezoelectric charge density

The piezoelectric polarization and stress are related by $P_i = d_{ijk}\sigma_{jk}$. Most elements of the piezoelectric tensor d_{ijk} vanish in GaAs because of its $\overline{4}3m$ symmetry.[21] The exceptions, in crystallographic axes, have $ijk = 123$ and permutations, all of which take the same value $\frac{1}{2}d_{14}$. Two rotations must be made to bring the tensor into our xyz axes. First is a rotation of θ about [100] which accounts for the direction in which current flows, taken as x. Second, we must rotate by π about x because our z-axis points downwards into the semiconductor. We then find that

$$P_x = -d_{14}\sigma_{xz}\sin 2\theta,$$

$$P_y = d_{14}\sigma_{xz}\cos 2\theta,$$

$$P_z = \tfrac{1}{2}d_{14}(\sigma_{yy} - \sigma_{xx})\sin 2\theta. \tag{3.1}$$

We can replace $\sigma_{yy} = \nu(\sigma_{xx} + \sigma_{zz})$ in a plane state of strain. The polarization field $\mathbf{P}$ can be replaced by a volume charge density $\rho = -\operatorname{div}\mathbf{P}$, which becomes

$$\rho(x,z) = \tfrac{1}{2}d_{14}\sin 2\theta\left[2\frac{\partial\sigma_{xz}}{\partial x} + (1-\nu)\frac{\partial\sigma_{xx}}{\partial z} - \nu\frac{\partial\sigma_{zz}}{\partial z}\right]. \tag{3.2}$$

The contribution from P_y has vanished to leave a characteristic dependence on $\sin 2\theta$. We can remove $\partial\sigma_{xz}/\partial x$ by using the condition $\operatorname{div}\sigma = 0$ for mechanical equilibrium.

Charges also appear at surfaces and interfaces. These are (just) smaller for our example and will be discussed in Sec. III D.

Next, we express the stress in terms of the harmonic function ϕ. The result is

$$\rho(x,z) = \tfrac{1}{2}d_{14}\sin 2\theta[(5-2\nu)\phi'' + 3z\phi'''] \tag{3.3}$$

$$= \tfrac{1}{2}d_{14}\sin 2\theta\sum_{n=1}^{\infty}q_n^2\phi_n[(5-2\nu) - 3q_n z]$$

$$\times\cos(q_n x)\exp(-q_n z), \tag{3.4}$$

where primes indicate derivatives with respect to z. The next step is to integrate Poisson's equation with this charge density, but we must first review the boundary conditions.

B. Boundary conditions for electrostatics

We expect the potential to vanish far from the gate, at $z \to \infty$, and this provides one boundary condition for Poisson's equation. A second is provided by the surface of the semiconductor and two simplified models were discussed in paper I. It is generally assumed that a high density of surface states pins the Fermi level at an almost constant energy on the surface of GaAs at room temperature, and the surface therefore acts as an equipotential. Pinning requires equilibrium to be maintained between the surface states and the

2DEG below, a process that must become very slow at low temperature. Then it may be more accurate to treat the charge in the surface states as frozen because it does not have time to adjust during an experiment. The surface now behaves as a simple dielectric boundary.

We have assumed that the strain arises from differential contraction between the gate and semiconductor, and therefore develops gradually as the sample is cooled. Moreover, much of the contraction occurs at higher temperatures where the surface states are active. We therefore take the surface to be pinned in the calculation of the static piezoelectric potential, and treat it as an equipotential at zero.

A conventional modulation-doped sample has a layer of donors between the surface and 2DEG. This can be ignored if all donors are ionized, but silicon in $Al_xGa_{1-x}As$ does not behave in such a simple way. Only about half the donors are ionized in a typical sample, the remainder being neutralized as DX centers.[22] The occupation of these donors is frozen below $T_F \approx 150$ K, but they act to screen the electrostatic potential above this temperature. The donors therefore act like another equipotential layer at $z = c$ if most of the piezoelectric charge density is developed above T_F. We suspect that this is often the case in structures used for physics experiments but probably not for practical transistors, which usually have a recessed gate to eliminate parasitic electrons around the donors. There may, however, be a slow relaxation of the piezoelectric potential if the donors or surface states have not come into equilibrium before an experiment is started.

The shallow δ-doped layer used in the experiment studied in paper I was unusual because it had AlAs barriers, and the donors were surrounded by a parasitic channel of electrons which remained free even at low temperature.[13] In this case it is certainly appropriate to treat the donors as an equipotential plane.

C. Potential energy in the 2DEG

We can now integrate Poisson's equation $\nabla^2\psi = -\rho/\epsilon\epsilon_0$ to find the piezoelectric potential ψ, with the charge density given by Eq. (3.4). We shall assume that the donors act as a zero equipotential, giving the boundary condition $\psi(z=c) = 0$; setting $c = 0$ returns the equipotential to the surface of the semiconductor if this is not the case. Again we expand the potential as a Fourier series, $\psi(x,z) = \Sigma_n\psi_n(z)\cos(q_n x)$, and find

$$\psi_n(z) = \frac{d_{14}\sin 2\theta}{8\epsilon\epsilon_0}q_n(z-c)[7-4\nu-3q_n(z+c)]\phi_n$$

$$\times\exp(-q_n z). \tag{3.5}$$

The bare potential energy for electrons in the 2DEG is given by $-e\psi(z=d)$, which is then screened by the 2DEG. The nearby equipotential plane provided by the donors (or surface) makes screening less effective at long wavelengths than for an isolated 2DEG.[23] This is taken into account by the modified Thomas-Fermi dielectric function introduced in paper I,

$$\epsilon_{TF}(q,p) = 1 + \frac{2}{a_0 q}[1 - \exp(-2qp)]. \tag{3.6}$$
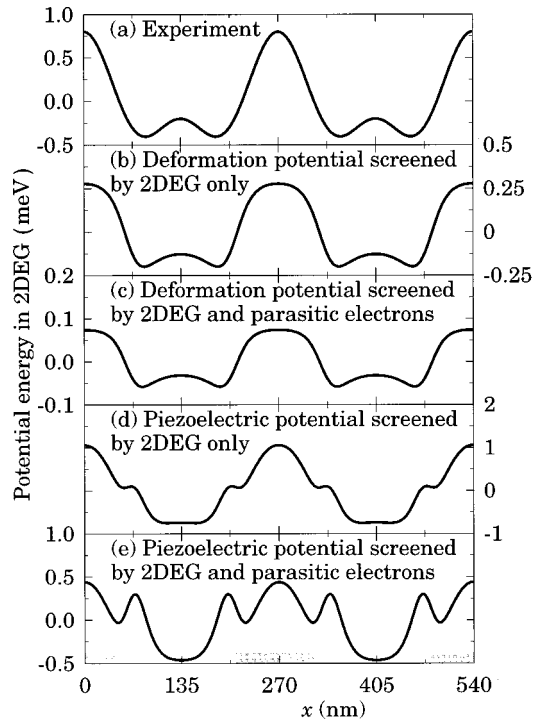
FIG. 3. Potential energy in the 2DEG under a lateral surface superlattice, whose gates are shown as gray rectangles. (a) Deduced from experiment (Ref. 7) the phases of the Fourier components are unknown. Curves (b)–(e) show calculations of the potential induced by strain, assuming a rigid gate giving compression of $\varepsilon_{xx}^{0} = -0.001$ on the surface of the semiconductor. Note the different scales.

In our case the equipotential plane is at a distance $p = d - c$. The Fourier coefficients of the potential energy induced in the 2DEG become

$$v_n = -\frac{e d_{14} \sin 2\theta}{8 \epsilon \epsilon_0} \frac{q_n(d-c)}{\epsilon_{TF}(q_n, d-c)} [7 - 4\nu$$
$$- 3q_n(d+c)] \phi_n \exp(-q_n d). \qquad (3.7)$$

This is our final expression for the Fourier expansion of the piezoelectric potential energy. Set $c = 0$ if the donors do not act as an equipotential.

An important point is that charge both above and below the 2DEG contributes to the potential. Screening from electrons around the donors therefore has less effect than it does on the deformation potential or an electrostatic potential from the gate. The numerical results make this clear.

D. Charge density at interfaces

The calculation above has only included the volume charge density. Discontinuities in the polarization also generate a charge density $\Delta \mathbf{P} \cdot \mathbf{n}$ at surfaces and interfaces. We find that these are smaller in the structure that we have used as an example, but this may not always be the case.

Our assumption of a pinned surface means that we can neglect any charge density here. Effectively we assume that the surface states absorb the piezoelectric charge without significant change of the Fermi level.

Charge may build up at interfaces within the heterostructure due to differences in the elastic, piezoelectric, or dielec-
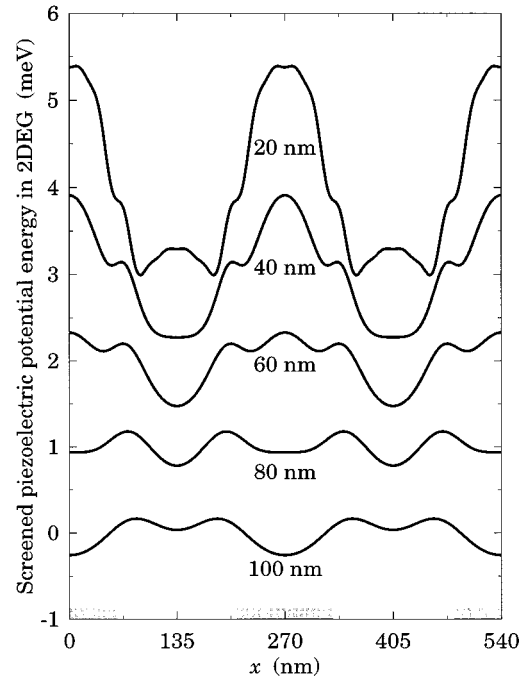
FIG. 4. Screened piezoelectric potential for different depths of the 2DEG. Screening by electrons around the donors is neglected, other parameters are as in Fig. 3, and successive curves are offset by 1 meV.

tric constants. This may be important because the 2DEG is trapped at an interface, and the charge here would be particularly effective.

The differences in elastic, dielectric, and piezoelectric constants between GaAs and AlAs (Ref. 20) are roughly 2%, 20%, and 40%, so the discontinuity in the piezoelectric constant is most significant. We estimate that this gives rise to about 4×10^{13} m^{-2} electrons at the interface with the 2DEG in the fundamental wavevector. This is about 1% of the density of the 2DEG so the induced potential energy is a similar fraction of the Fermi energy or about 0.1 meV. This is smaller than the potential from the space charge but only by a factor of 3 or so. We shall not consider it further in this paper, and we shall also neglect the discontinuity in the elastic and dielectric constants whose effects will be smaller. Interface charges are more significant in other heterostructures where the properties of the materials are more distinct.

IV. RESULTS

The results of our calculations of the potential energy in the 2DEG under a lateral surface superlattice are plotted in Figs. 3–6, and the first three harmonics are summarized in Table I. Again we used parameters to match the device[7] studied in paper I, and most of the calculations are for a rigid gate with $\varepsilon_{xx}^{0} = -0.001$ underneath. The plane of donors with a parasitic channel of electrons in this device is treated as an equipotential. Current flowed along a $\langle 011 \rangle$ direction so we set $\theta = 45°$, which maximizes the piezoelectric potential. We use parameters for GaAs (Ref. 20) of $\epsilon = 13.2$, $d_{14} = -2.69 \times 10^{-12}$ CN^{-1}, and $\Xi = -8.2$ eV throughout. A small inaccuracy arises because most of the material between the 2DEG and the surface is usually
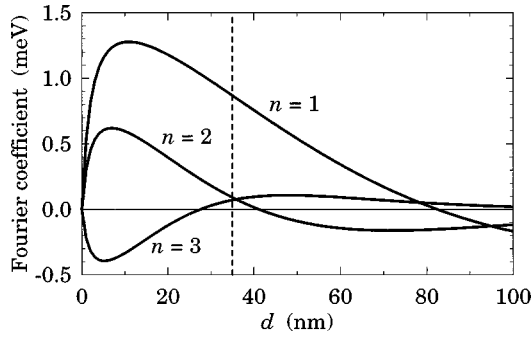
FIG. 5. First three harmonics of the screened piezoelectric potential as a function of the depth of the 2DEG. Screening by electrons around the donors is neglected and other parameters are as in Fig. 3. The broken line marks the depth of the 2DEG used in the plots for Fig. 3.

$Al_xGa_{1-x}As$ (or AlAs in the experiment studied here). The piezoelectric charge also extends below the 2DEG, however, which reduces the error.

A. Deformation and piezoelectric potentials

The deformation and piezoelectric potentials calculated for this device are compared in Fig. 3. The piezoelectric potential is about four times stronger than the deformation potential, and has a higher harmonic content, when only screening by the 2DEG is included. Further screening due to electrons around the donors reduces the deformation potential by a factor of about 4. The piezoelectric potential is reduced to about 40% of its previous value and its harmonics are further emphasized.

Figure 4 shows the screened piezoelectric potential as a function of the depth of the 2DEG, other parameters remaining unchanged. Screening due to electrons around the donors is omitted for clarity. The potential decays with increasing depth, as expected, but there is also a striking change in harmonic content. The fundamental component passes through zero and changes sign around 80 nm. This is con-
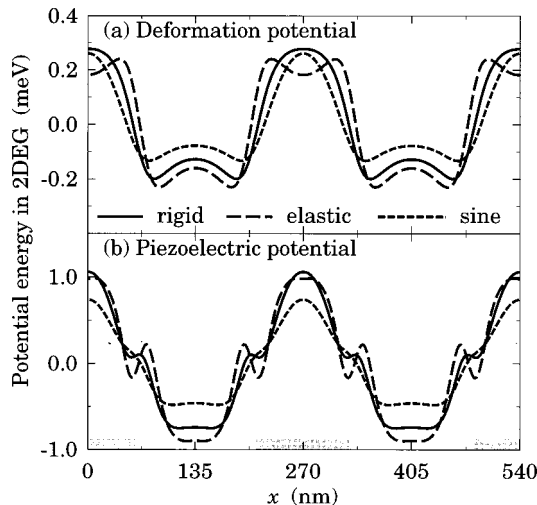
FIG. 6. Comparison of screened deformation and piezoelectric potentials under rigid, elastic, and sine gates. Screening by electrons around the donors is neglected and other parameters are as in Fig. 3.

firmed by the plot of Fourier coefficients [Eq. (3.7)] as a function of depth in Fig. 5. A small change in the ratio of depth to period clearly has a substantial influence on the piezoelectric potential. The periodic modulation is maximized at a depth of about 10 nm which is unfortunately too shallow to be practicable. The change in sign follows immediately from Eq. (3.7) and the critical depth depends mainly on the period of the gates. In principle a device could be made with no first harmonic in the piezoelectric potential.

In contrast, the bare deformation potential is proportional to the dilation. This is a harmonic function[14] so each Fourier component decays exponentially as $\exp(-q_n d)$. Thus the relative amplitudes of the harmonics changes but their signs do not. Screening has only a small effect on this.

B. Different elastic models

Figure 6 shows the deformation and piezoelectric potentials for the elastic, rigid, and sine models of the gate, screened by the 2DEG alone. Figure 2 showed that the stress was of similar magnitude in all three models and this is reflected in the electronic potentials. In contrast, the harmonic content of the potentials is sharply different, confirmed by Table I. This follows from the nature of the Fourier series for the elastic function ϕ (Sec. II B), as the device is close to the limit $a=b$. The curves for the elastic gate therefore show a symmetry between the gates and gaps, giving a small second harmonic and a large third one. Both the rigid and sine gates show a stronger second harmonic but the third harmonic is different; it is much weaker for the sine gate but almost as strong as the second harmonic for the rigid gate.

C. Comparison with experiment

Figure 3(a) shows the potential deduced from experiment.[7] The significant features are its magnitude, the strong second harmonic, and absence of a third harmonic within experimental resolution. It is compared with calculations using a rigid gate.

Qualitatively, the closest match to experiment is offered by the deformation potential screened by the 2DEG alone [Fig. 3(b)]. This has the observed strong second harmonic but the third harmonic is noticeable too. Its magnitude is too small by a factor of two but our estimate of the strain may well contain such an error. The main problem is that this result takes no account of the mobile electrons around the donors revealed by other experiments.[13] The inclusion of these reduces the potential to that in Fig. 3(c) which is too small by nearly an order of magnitude.

In contrast, the piezoelectric potential has about the right magnitude, even when screening by electrons around the donors is included [Fig. 3(e)]. Unfortunately the harmonic content agrees much less well, with an excessively strong third harmonic. However, Figs. 4 and 5 show that the strength of the harmonics is a rapidly varying function of the dimensions of the device. A small error resulting from, say, lack of adhesion of the edge of the gates, would have a large effect on the harmonic content. Indeed a reduction in a improves the agreement with experiment.

These calculations, like those in paper I, employed a rigid gate. The elastic gate might seem more appropriate as the

TABLE I. The first three harmonics of the potential in the 2DEG observed in experiment (Ref. 7) and calculated from strain using different models. Under ''Screening,'' ''2DEG'' means that the potential is screened by the 2DEG alone, while ''parasitic'' includes additional screening by electrons around the donors.

Gate	Coupling	Screening	v_1 (meV)	v_2 (meV)	v_3 (meV)
	experiment		± 0.5	± 0.3	< 0.1
rigid	deformation	bare	1.9	0.49	-0.16
rigid	deformation	2DEG	0.24	0.10	-0.04
rigid	deformation	parasitic	0.064	0.028	-0.013
rigid	piezoelectric	bare	6.9	0.47	0.28
rigid	piezoelectric	2DEG	0.87	0.091	0.072
rigid	piezoelectric	parasitic	0.36	-0.10	0.13
elastic	deformation	bare	2.0	0.10	-0.38
elastic	deformation	2DEG	0.25	0.02	-0.10
elastic	deformation	parasitic	0.055	0.005	-0.028
elastic	piezoelectric	bare	7.1	0.10	0.66
elastic	piezoelectric	2DEG	0.90	0.02	0.17
elastic	piezoelectric	parasitic	0.38	-0.02	0.30
sine	deformation	bare	1.3	0.53	0.020
sine	deformation	2DEG	0.16	0.10	0.005
sine	deformation	parasitic	0.037	0.026	0.002
sine	piezoelectric	bare	4.8	0.51	-0.035
sine	piezoelectric	2DEG	0.60	0.10	-0.009
sine	piezoelectric	parasitic	0.25	-0.10	-0.016

thickness of the gates, 30 nm, is much smaller than their length of 130 nm. However, Fig. 6 and Table I show that the harmonics predicted from this model agree much less well with experiment.

The best agreement is obtained with the sine gate. It has large first and second harmonics but a very small third harmonic, and its magnitude is about right. This success is slightly surprising, given that it is a very rough solution to the elastic equations. We suspect that the reason lies in the way in which the force between the gate and semiconductor is distributed near the edges of the gate. The elastic model, which might have been expected to be most appropriate, has the force concentrated into a δ function at each end. In practice it is more realistic to spread the force over a width similar to the thickness. Furthermore, it is often difficult to obtain good adhesion of the edges of a gate, and it is likely that relaxation (perhaps even debonding) occurs to spread this force over a wider area. This may explain why the rigid and sine gates work better. An even more extreme model would be a purely cohesive interface with $P_x(x) \propto \text{sign } x$. It might be difficult to treat relaxation even with numerical modeling, and the success of the sine model shows that the effects may be large.

We conclude that the piezoelectric effect is the more likely explanation of the observations, but that it is difficult to resolve the source of the periodic potential from its functional form alone. An obvious distinction between the deformation and piezoelectric potentials is their dependence on orientation. The deformation potential does not depend on θ, within the validity of the isotropic approximation for the elastic fields. The piezoelectric potential, in contrast, varies as $\sin 2\theta$ and changes sign between the two common directions of current, [011] and [01$\bar{1}$]. This dependence has been

seen in a recent experiment[12] which confirms the piezoelectric effect as the dominant source of the periodic potential under an unbiased lateral surface superlattice. This experiment used a gate bias to cancel the built-in potential and detect its sign. Unfortunately we predict the opposite sign. We do not at present understand this. If the discrepancy cannot be traced to an error in our calculation or the experiment, or an ambiguity in the definition of the orientation or piezoelectric constant, we must conclude that the GaAs is in tension rather than compression under each gate. This would imply an origin other than thermal expansion. An independent experiment to measure the stress under a metal gate, or to apply a better defined stress, would be welcome.

V. CONCLUSIONS

Our calculations show that the piezoelectric effect provides the dominant interaction between strain under a lateral surface superlattice and the electrons in a 2DEG for devices in the conventional orientation on GaAs. The magnitude is in good agreement with experiment.[7] Although the harmonic content is predicted less well, the model used for the elastic behavior of the gate has a large effect. The harmonics are also sensitive to small errors in the input parameters. Direct confirmation comes from the dependence on orientation.[12] Screening by electrons around the donors has less of an effect than it does on the deformation potential, because much of the piezoelectric charge is deeper than the 2DEG.

We have considered elastic and rigid approximations for the behavior of the gate with an intermediate ''sine'' model. A thin gate should be nearer the elastic limit but we find that the results are closer to experiment using a sine gate, with a roughly linear shear profile underneath. A rigid gate lies in

between. We speculate that the predictions using the sine gate are successful because of relaxation, or perhaps lack of adhesion, at the edges of the gates.

An improved theory of strain would probably have to abandon the isotropic approximation for the elastic problem, which is not particularly accurate for the III–V semiconductors. The isotropy ratio $S = (c_{11} - c_{12})/2c_{44} = 0.55$ for GaAs (Ref. 20), which is far from its limit of unity in an isotropic medium. Unfortunately an analytic solution may be possible only for special orientations if cubic symmetry is retained.

We have also shown that unfamiliar sources of screening should be taken into account, notably the surface and electrons around donors in $Al_x Ga_{1-x} As$. Both the potential due to strain and the screening from these regions are functions of time as a sample is cooled to cryogenic temperature. The final potential energy may therefore depend on the history of a sample as well as its construction. Relaxation of the potential may also occur as the surface or donors slowly approach equilibrium.

A further source of screening which we have not included is provided by the doping of the substrate. This could be modeled with another equipotential plane at the edge of the depletion layer. Modern heterostructures for physics experiments usually have such a low doping in the substrate that the effect is negligible, but it may be significant in a field-effect transistor on a doped buffer layer. A back gate formed by a buried conducting layer would have a similar effect.

Our work carries two main implications for experiments. If modulation of the potential under a gate is *not* required, the device should be aligned parallel to a crystallographic axis. The deformation potential remains, as does any built-in voltage, but this orientation eliminates the largest effect.

Where the aim is to influence the electrons as strongly as possible, the potential can be enhanced by the growth and patterning of stressors. This technique has a long history in waveguides[15] and the confinement of excitons.[24,25] Much larger stresses and potentials can be generated that we have shown here; for example, the stress in overlayers of Si_3N_4 can reach[10] 10^9 N m^{-2}, an order of magnitude higher than in our gate. Clearly there is great scope for developing the piezoelectric effect to guide or confine carriers in a heterostructure.

*Present address: Department of Physics, Sheffield University, Sheffield, S3 7RH, U. K.

†Electronic address: jdavies@elec.gla.ac.uk

[1] C. W. J. Beenakker and H. van Houten, *Solid State Physics: Advances in Research and Applications*, edited by H. Ehrenreich and D. Turnbull (Academic Press, Boston, 1991), Vol. 44, p. 1.

[2] D. Weiss, K. von Klitzing, K. Ploog, and G. Weimann, Europhys. Lett. **8**, 179 (1989).

[3] R. R. Gerhardts, D. Weiss, and K. von Klitzing, Phys. Rev. Lett. **62**, 1173 (1989).

[4] R. W. Winkler, J. P. Kotthaus, and K. Ploog, Phys. Rev. Lett. **62**, 1177 (1989).

[5] C. W. J. Beenakker, Phys. Rev. Lett. **62**, 2020 (1989).

[6] R. R. Gerhardts, Phys. Rev. B **45**, 3449 (1992).

[7] R. Cuscó, M. R. Holland, J. H. Davies, I. A. Larkin, E. Skuras, A. R. Long, and S. P. Beaumont, Surf. Sci. **305**, 643 (1994); R. Cuscó, E. Skuras, S. Vallis, M. C. Holland, A. R. Long, S. P. Beaumont, I. A. Larkin, and J. H. Davies, Superlattices Microstruct. **16**, 283 (1994).

[8] J. H. Davies and I. A. Larkin, Phys. Rev. B **49**, 4800 (1994).

[9] See, for example, P. D. Ye, D. Weiss, R. R. Gerhardts, K. von Klitzing, K. Eberl, H. Nickel, and C. T. Foxon, Semicond. Sci. Technol. **10**, 715 (1995).

[10] P. M. Asbeck, C.-P. Lee, and M.-C. F. Chang, IEEE Trans. Electron Devices **31**, 1377 (1984).

[11] L. Cong, J. D. Albrecht, M. I. Nathan, P. P. Ruden, and D. L. Smith, Appl. Phys. Lett. **66**, 1358 (1995).

[12] E. Skuras, A. R. Long, I. A. Larkin, J. H. Davies, and M. C. Holland, Appl. Phys. Lett. **70**, 871 (1997).

[13] E. Skuras, M. C. Holland, C. J. Barton, J. H. Davies, and A. R. Long, Semicond. Sci. Technol. **10**, 922 (1995).

[14] L. D. Landau, E. M. Lifshitz, A. M. Kosevich, and L. P. Pitaevskii, *Theory of Elasticity* (Pergamon, Oxford, 1986).

[15] P. A. Kirkby, P. R. Selway, and L. D. Westbrook, J. Appl. Phys. **50**, 4567 (1979).

[16] I. A. Blech and E. S. Meieran, J. Appl. Phys. **38**, 2913 (1967).

[17] See, for example, H. M. Westergaard, *Theory of Elasticity and Plasticity* (Harvard University Press, Cambridge, MA, 1952).

[18] J.-C. Ramirez, P. J. McNally, L. S. Cooper, J. J. Rosenberg, L. B. Freund, and T. N. Jackson, IEEE Trans. Electron Devices **35**, 1232 (1988).

[19] See, for example, W. R. Smythe, *Static and Dynamic Electricity* (McGraw Hill, New York, 1950).

[20] S. Adachi, J. Appl. Phys. **58**, R1 (1985).

[21] J. F. Nye, *Physical Properties of Crystals* (Oxford University Press, Oxford, 1957).

[22] P. M. Mooney, Semicond. Sci. Technol. **6**, B1 (1991).

[23] A different treatment of screening under a superlattice is given by C. Nguyen, B. Brar, V. Jayaraman, A. Lorke, and H. Kroemer, Appl. Phys. Lett. **63**, 2251 (1993).

[24] K. Kash, R. Bhat, D. D. Mahoney, P. S. D. Lin, A. Scherer, J. M. Worlock, B. P. Van der Gaag, M. Koza, and P. Grabbe, Appl. Phys. Lett. **55**, 681 (1989).

[25] I.-H. Tan, D. Lishan, R. Mirin, V. Jayaraman, T. Yasuda, E. L. Hu, and J. Bowers, Appl. Phys. Lett. **59**, 1875 (1991).